

# Structural transitions and thermally averaged infrared spectra of small methanol clusters

U. Buck, B. Schmidt,<sup>a)</sup> and J. G. Siebers

Max-Planck-Institut für Strömungsforschung, D 37073 Göttingen, Federal Republic of Germany

(Received 29 June 1993; accepted 30 August 1993)

Classical Monte Carlo and molecular dynamics (MD) simulations were carried out to investigate the structures, the infrared spectra, and the rigid–nonrigid transitions of small methanol clusters  $(\text{CH}_3\text{OH})_n$  for  $n=3$ –6. The study was motivated by experimental results for these clusters from size specific infrared (IR) dissociation spectroscopy. The MD simulations revealed the following transitions: The trimer passes from a rigid ring configuration into a series of nonrigid open chain structures starting at 197 K. For  $n=4$  and 5 such transitions occur between rings and rapidly fluctuating ring structures at  $T=357$  and 243 K, respectively. For  $n=6$  first a pure isomeric transition between the two energetically lowest isomers of  $S_6$  and  $C_2$  symmetry is found at 35 K, and then a similar transition to a nonrigid behavior as is observed for  $n=4$  and 5 is seen at 197 K. The measured spectra display in all cases the rigid lowest energy configurations.

## I. INTRODUCTION

The nature of phase transitions in finite systems and especially the applications to clusters have attracted much interest in recent years. The great majority of the investigations have been carried out by computer simulations and some general concepts emerged connected with the names of Berry, Jortner, and co-workers.<sup>1–4</sup> The “melting” of clusters is, in general, described as isomerization between a multitude of isomers. The gross features of the size and temperature dependence of this cluster isomerization crucially depends on their interaction and their chemical properties. Weak short range interactions in rare gas clusters like  $\text{Ar}_n$  lead to a large number of isomers and phase transitions occur preferentially between the lowest energy configurations, usually belonging to an icosahedral growth sequence, and the many other isomers leading to a transition temperature range in which both, a solidlike and a liquidlike “phase,” are present. Strong long range interactions in alkali halide clusters involve isomerization between a very small number of well characterized isomers, a nice example being the cube→ring transition of  $(\text{NaCl})_4$ .<sup>5,6</sup> Similar results have been obtained for  $(\text{KCl})_n$  clusters.<sup>7</sup> In both binding types the melting temperature decreases with decreasing cluster size and is lower than the bulk value, a result which was also observed experimentally for metallic clusters supported on a substrate<sup>8</sup> and which can be rationalized by thermodynamical arguments.

A somewhat different result has been obtained for heteroclusters which consist of an aromatic molecule which is embedded in or on a rare gas cluster.<sup>9</sup> Here an occurrence of several hierarchical isomerization phenomena was observed, i.e., correlated surface motion, surface melting, side crossing, wetting–nonwetting, and rigid–nonrigid transitions.<sup>10</sup> In contrast to what has been seen so far, the temperature onsets of most of these transitions are not uniform

or tend to decrease with increasing cluster size reflecting finite microsurface effects.<sup>11</sup>

Systematic investigations of the size dependence of phase transitions for neat molecular clusters have, aside from one exception for small  $(\text{CO}_2)_n$  clusters from  $n=3$  to 13,<sup>12</sup> not been performed. In simulations of  $(\text{C}_6\text{H}_6)_4$  (Ref. 13) and of  $(\text{H}_2\text{O})_8$  (Ref. 14) the temperatures of the rigid→nonrigid transition were found to be considerably lower than those associated with the bulk material. Similar results have been obtained for large  $(\text{CCl}_4)_n$ ,<sup>15</sup>  $(\text{H}_2\text{O})_n$ ,<sup>16</sup>  $(\text{SF}_6)_n$ ,<sup>17</sup> and  $(\text{CO}_2)_n$  (Refs. 22 and 23) clusters.

Experimental information on these phase transitions is difficult to get. Electron diffraction studies provide results on temperatures and structures.<sup>18,19</sup> The spectroscopic interrogation of the vibrational<sup>20,21,24</sup> and electronic<sup>9–11,25</sup> excitation of homogeneous clusters or guest molecules in heteroclusters attracted considerable attention. In case of the infrared (IR)-spectra the simulations revealed detailed dependences on the local structure, the surface and interior states as well as melting phenomena. The experiments, however, are performed with a distribution of cluster sizes<sup>26</sup> so that accurate conclusions cannot be drawn. In case of electronic excitation, the size dependence of the spectroscopic line broadening was interpreted in terms of cluster isomerization phenomena. Detailed simulations, however, showed that the gradual line narrowing can, in some cases, be attributed to a combined effect of homogeneous line broadening and the isomer specificity of spectral shifts.<sup>10,11,25</sup> Single isomers, however, are identified by their spectral and ionization potential shifts and their radiative lifetimes.

In this contribution, we will present Monte Carlo (MC) and molecular dynamics (MD) simulations both of the temperature dependence of infrared spectra and the isomeric transitions of small homogeneous methanol clusters from the dimer to the hexamer. This choice was motivated by the fact that for these systems infrared spectra were measured in the region of the CO-stretching mode for size selected clusters.<sup>27,28</sup> In addition, methanol plays an

<sup>a)</sup>Present address: The Fritz Haber Research Center for Molecular Dynamics, The Hebrew University of Jerusalem, Jerusalem 91904, Israel.

important role as a polar solvent with a linear hydrogen bond which is different from water. Because of the two lone pair orbitals and two H-atoms the coordination number in the condensed phases of water is near 4, while the phases of solid methanol are known to be made up of parallel hydrogen bonded chains with coordination number 2. Similarly, the dominating structures of liquid methanol are long winding chains with occasional branching points. On the other hand, it is well known that thermodynamic properties in the gas phase like the thermal conductivity clearly demonstrate the existence of larger clusters in ethanol vapor.<sup>29</sup>

In the following, we first summarize the model used for calculating the structure and the frequency shifts of the vibrational spectra. We then describe the simulation techniques, present the spectra as a function of temperature, compare the results with experiments, and show some remarkable changes which can be associated with isomerization. In the final section these phase transitions are further investigated by their caloric curves, relative bond length fluctuations, and their time dependent mean square displacements.

## II. DETAILS OF THE SIMULATIONS

### A. The methanol pair potential

The most basic requirement for simulations of structural as well as spectroscopic properties of clusters is the choice of a realistic interaction potential. Since *ab initio* calculations for the systems considered here are still extremely expensive, we use the empirical optimized potential for liquid simulations (OPLS) designed by Jorgensen.<sup>30</sup> It was derived by fitting a simple potential function to various thermodynamic and structural data of liquid alcohols. In this model each methanol molecule is represented by three potential sites placed at the positions of the hydroxyl H atom, the O atom, and the methyl group, respectively. Then the total interaction energy is calculated by summing up all pairwise site-site interactions. The isotropic potential between each pair of sites  $i$  and  $j$  as a function of their distance  $r_{ij}$  is given by the sum of a Coulomb and a Lennard-Jones 12-6 term

$$V_{ij} = \frac{1}{4\pi\epsilon_0} \frac{q_i q_j}{r_{ij}} + \frac{A_{ij}}{r_{ij}^{12}} - \frac{C_{ij}}{r_{ij}^6}. \quad (1)$$

The parameters  $A_{ij}$  and  $C_{ij}$  describing the interaction of the sites  $i$  and  $j$  can be calculated using the empirical combination rules

$$A_{ij} = \sqrt{A_i A_j}$$

and

$$C_{ij} = \sqrt{C_i C_j} \quad (2)$$

from the parameters  $A_i$  and  $C_i$  which are easily obtained from the Lennard-Jones parameters  $\epsilon_i$  and  $\sigma_i$  using the relations

$$A_i = 4\epsilon_i \sigma_i^{12}$$

and

TABLE I. Potential parameters of the OPLS model of methanol.

	$q_i/c$	$\sigma_i/\text{pm}$	$\epsilon_i/\text{kJ mol}^{-1}$
CH <sub>3</sub>	+0.265	384	0.799
O	-0.700	307	0.711
H	+0.435	...	...

$$C_i = 4\epsilon_i \sigma_i^6. \quad (3)$$

The values of the OPLS potential parameters  $q_i$ ,  $\epsilon_i$ , and  $\sigma_i$  are summarized in Table I. The predicted minimum energy structures obtained for this potential model are discussed in our previous study on structure and infrared spectra of small methanol aggregates.<sup>32</sup> In that study the OPLS model is also compared with other interaction potentials. Here, we only present a brief review of the main structures in Sec. III A.

Calculations have been performed to test the sensitivity of the conclusions of the paper to the potential model used. We utilize the intermolecular potential of Ref. 33 which will be referred to as PHH3. This PHH3 potential uses a combination of exponential and power law dependencies for all atomic interactions. It gives a better description of the dimer properties than OPLS, which did not take account of interactions of the two H atoms.

### B. Monte Carlo simulations

With increasing temperatures a cluster can explore wider and wider regions of its configurational space. One technique to simulate this process of thermal averaging is the classical MC integration over the accessible phase space. For a given temperature and a given number of particles a canonical distribution of cluster configurations is generated using the standard "random walk" algorithm.<sup>34</sup> Assuming the molecules to be rigid, their positions and orientations are described by six coordinates, three Cartesian coordinates  $x, y, z$  specify the position of the center of mass and three Euler angles  $\phi, \theta, \psi$  give the orientation of each molecule.<sup>35</sup> Using this set of coordinates, a Monte Carlo move is defined by the following equations:

$$\begin{aligned} x_n &= x_o + 2(\xi_1 - 1)\delta r_{\max}, & y_n &= y_o + 2(\xi_2 - 1)\delta r_{\max}, \\ z_n &= z_o + 2(\xi_3 - 1)\delta r_{\max}, & \phi_n &= \phi_o + 2(\xi_4 - 1)\delta\phi_{\max}, \\ \cos \theta_n &= \cos \theta_o + 2(\xi_5 - 1)\delta(\cos \theta)_{\max}, \\ \psi_n &= \psi_o + 2(\xi_6 - 1)\delta\psi_{\max}, \end{aligned} \quad (4)$$

where the indices  $n$  and  $o$  stand for "new" and "old,"  $\xi_i$  are random numbers from a uniform distribution over the interval  $[0, 1]$ , and  $\delta r_{\max}$ ,  $\delta\phi_{\max}$ ,  $\delta(\cos \theta)_{\max}$ , and  $\delta\psi_{\max}$  are the maximum sizes of the attempted moves in the respective coordinates. Note that in the fifth equation we increment  $\cos \theta$  instead of  $\theta$  in order to sample uniformly the orientational space spanned by the Euler angles.<sup>36</sup> A ca-

nonical distribution is constructed from the so defined moves applying the usual criterion for the acceptance of the random moves. A new configuration is always accepted if the change in potential energy  $\Delta E$  associated with this move is negative, or else it is accepted with a probability of  $\exp(-\Delta E/k_B T)$ , where  $T$  is the temperature and  $k_B$  is the Boltzmann constant.

In this way Monte Carlo simulations are carried out for methanol clusters ranging from the trimer to the hexamer. The initial configurations for the runs are the energetically lowest configuration of each of the aggregates as discussed in Sec. III A. The maximum widths are chosen such that  $\sim 50\%$  of the attempted moves are accepted. Typically, thermal equilibrium is reached after  $10^4$ – $10^5$  MC steps. Then ensemble averages are obtained over the next  $10^6$  steps of the simulation runs. To guarantee statistical independence, only every 100th configuration is included in the process of averaging.

### C. Molecular dynamics simulations

Classical, constant energy MD simulations were carried out for cluster sizes  $n=3, 4, 5, 6$ , and a range of total energies. The molecules were treated as rigid rotors, splitting the equations of motion into translational and rotational ones. Since the Eulerian equations of motion possess singularities at  $\theta=0, \pi$ ,<sup>35</sup> they are inadequate for use in a numerical integration scheme. For MD simulations Evans first introduced the quaternion parameters giving singularity-free expressions.<sup>36–38</sup> We follow this approach using a Gear fifth- and sixth-order predictor-corrector algorithm for the integration of the translational and rotational equations of motion, respectively.<sup>39</sup>

A time step of 0.6 fs was chosen for runs of  $10^6$  steps length or 0.6 ns. The noise and drift<sup>40</sup> of the total energy under these conditions were  $\leq 0.3\%$  and  $\leq 0.05\%$  per ns for all simulations, respectively. For a given cluster size a simulation series consisted of the following parts: (1) Choice of initial conditions. The lowest minima positions of  $(\text{CH}_3\text{OH})_n$  found in Ref. 32 were slightly distorted from their equilibrium configurations and used for the first simulation of a series. Note that the distortion from the equilibrium structures is essential in the procedure for the trimer and tetramer configurations since they are planar yielding only two-dimensional results otherwise. (2) Calibration. To calibrate the temperature of the simulation the velocities were periodically scaled to a reference temperature  $T_r$  every 400 time steps which was repeated 30 times. The last phase space point of a simulation served as an input for the next one in a series.  $T_r$  was changed by 2 K from simulation  $j$  to  $j+1$ . (3) Equilibration. The systems were allowed another 12 000 time steps to relax and reach their thermal equilibrium. (4) Evaluation of relevant phase space points. After equilibration every tenth time step was used to calculate the quantities of interest.

Thus thermal equilibrium is reached after 12 ps and the runs are extended to 0.612 ns. The time scale of evaporation of a monomer from a hexamer cluster is estimated to be in the order of 50 ns for the temperature 300 K using the standard procedures of unimolecular decay.<sup>41</sup> There-

fore evaporation does not influence the calculated results. This is in qualitative agreement with the simulations in which no evaporation is observed.

### D. Ensemble averages

Having in mind the objective of finding and characterizing structural transitions for these clusters, the following quantities were calculated:

(1) While in the MC simulations the internal temperature  $T$  of the cluster can be chosen as a parameter, it is calculated in the MD calculations using the equipartition theorem. The internal temperature  $T$  of the cluster is then given by<sup>42–44</sup>

$$T = \frac{2}{6n-6} \frac{\langle E_{\text{kin}} \rangle}{k_B}, \quad (5)$$

where  $E_{\text{kin}}$  is the kinetic energy of the system,  $n$  is the number of molecules in the cluster,  $k_B$  is the Boltzmann constant, and  $\langle \rangle$  denotes an average over the whole trajectory. The temperature is given with the statistical error based on the 95%-confidence limit

$$\langle T \rangle = \frac{1}{m} \sum_{k=1}^m T_k \pm \alpha_m \frac{s}{\sqrt{m}}, \quad (6)$$

where

$$s = \sqrt{\frac{\sum_{k=1}^m \left( T_k - \frac{1}{m} \sum T_k \right)^2}{m-1}}, \quad (7)$$

$T_k$  is the temperature calculated over the  $m$ th part of the trajectory, and  $\alpha_m$  is the 0.975 fractile of Student's distribution for  $m$  observations.<sup>45</sup> The statistic was calculated for  $m=25, 30, 50$ , giving smallest uncertainties in  $T$  for  $m=50$  which are reported here.

(2) The relative root-mean-square (rms) bond length fluctuations  $\delta_{\text{cm}}$  (Refs. 42–44) of the centers of mass of the molecules

$$\delta_{\text{cm}} = \frac{2}{n(n-1)} \sum_{i < j} \frac{(\langle r_{ij}^2 \rangle - \langle r_{ij} \rangle^2)^{1/2}}{\langle r_{ij} \rangle}, \quad (8)$$

where  $r_{ij}$  is the distance between the centers of mass of molecule  $i$  and  $j$ . According to the Lindemann criterion<sup>46</sup> a substance undergoes melting when  $\delta$  reaches  $\sim 10\%$ .

(3) The distribution  $h(r)$  of distances  $r_i$  from the center of mass of molecule  $i$  to the center of mass of the cluster

$$h(r) = \left\langle \frac{1}{n} \sum_{i=1}^n \int_0^{r_i} \delta(r' - r) dr' \right\rangle, \quad (9)$$

where  $\delta$  denotes the Delta-function.

(4) The mean square displacements (MSD) of the center of mass positions  $r_i$  of the molecules as a function of time

$$\langle r(t)^2 \rangle = \frac{1}{n_{t_0}} \frac{1}{n} \sum_{j=1}^{n_{t_0}} \sum_{i=1}^n [\mathbf{r}_i(t_{0j} + t) + \mathbf{r}_i(t_{0j})]^2, \quad (10)$$

where  $n_{t_0}$  is the number of different time origins. Note that the slope of the MSD is directly proportional to the diffusion coefficient. Because this quantity is time dependent it cannot be obtained from the MC simulations.

### E. Infrared spectra

Besides the ensemble averages of structural properties much information about microclusters can also be gained from their spectra. In this work we restrict ourselves to the simulation of infrared spectra in the region of the  $\nu_8$  fundamental band of methanol. This vibrational band corresponds to excitation of the CO stretching mode. For free molecules this absorption lies at  $1033.5 \text{ cm}^{-1}$ .<sup>31</sup> In molecular clusters this frequency may be shifted and split due to the intermolecular forces. In experiments with size selected clusters frequency shifts in the order of  $\pm 20 \text{ cm}^{-1}$  were detected.<sup>27,28</sup>

In order to simulate these spectra we make use of a hybrid method. The intramolecular vibrations of the molecules constituting a cluster are treated by a quantum mechanical method while the thermal averaging over the intermolecular degrees of freedom is achieved using classical MC or MD procedures. This choice is justified by the fact that the intra- and intermolecular forces as well as the corresponding densities of states differ by several orders of magnitude. According to this hybrid scheme our procedure will be split into two different parts.

(1) We need a recipe to calculate the shifts of intramolecular vibration frequencies for a given configuration of the molecules in a cluster. Here we use a method based on degenerate perturbation theory. For details of this procedure the interested reader is referred to Ref. 32. The main idea is as follows: Assuming the amplitudes of the vibrational motions to be much smaller than the separations between the molecules, the intermolecular forces can be treated as a quantum mechanical perturbation acting on the normal mode vibrations of the molecules.<sup>47,48</sup> Coupling of vibrational modes of identical molecules is treated in first order perturbation theory for degenerate states. It leads to a splitting of the frequencies corresponding to the excitation of different collective modes of vibration of the complete cluster. These modes can be viewed as linear combinations of the respective normal modes of the constituent molecules. In the same way also transition dipole moments can be calculated as a vector sum of the moments of the individual molecules. Further corrections of the absorption frequencies are obtained in second order. In these formulas the inter/intramolecular coupling of vibrational modes plays an important role.<sup>49</sup> The required cubic force constants of the methanol molecule are taken from self-consistent field (SCF) *ab initio* calculations of Schlegel *et al.*<sup>50</sup>

(2) The spectral line shifts calculated with this procedure are then thermally averaged over a canonical or microcanonical distribution of cluster configurations which has been generated using MC or MD techniques, respectively, as described in the previous sections. For each of the molecular arrangements in the ensemble instantaneous

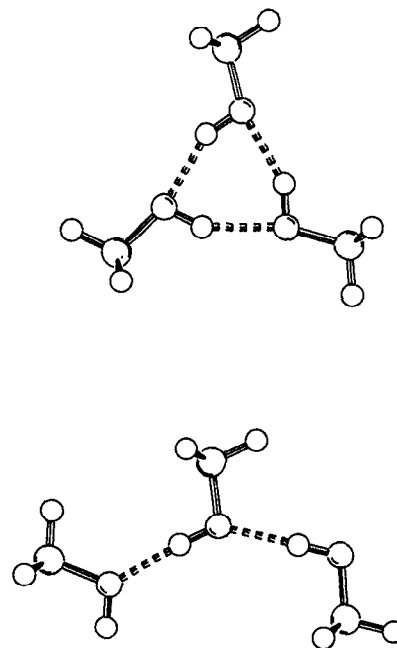


FIG. 1. Calculated minimum configurations of the methanol trimer. Upper panel, the lowest minimum structure of  $C_{3h}$  symmetry and a binding energy of  $\Delta E = -73.44 \text{ kJ/mol}$ . Lower panel, a chain structure with a binding energy of  $\Delta E = -59.47 \text{ kJ/mol}$ .

spectra are calculated using the above-mentioned perturbation scheme. The resulting absorption frequencies are binned into a histogram weighted with their appropriate infrared intensities which are proportional to the square of the respective transition dipole moment obtained in first order perturbation theory.

## III. RESULTS AND DISCUSSION

### A. Structural properties

In this section we give a brief discussion of the structural properties of the investigated methanol clusters using the OPLS potential. A more detailed description of the lowest energy configurations and some of the isomers of the hexamer is given in Ref. 32.

The methanol dimer is characterized by a linear  $\text{O-H}\cdots\text{O}$  hydrogen bond with an O-O distance of 274 pm and a binding energy of  $\Delta E = -28.53 \text{ kJ/mol}$  using the OPLS potential model. For the trimer only six minimum configurations were found, one ring ( $r$ ) and five chainlike ( $c$ ) structures. The binding energies of  $\Delta E = -73.44 \text{ kJ/mol}$  ( $r$ ),  $-62.80 \text{ kJ/mol}$  ( $c$ ),  $-62.63 \text{ kJ/mol}$  ( $c$ ),  $-59.93 \text{ kJ/mol}$  ( $c$ ),  $-59.47 \text{ kJ/mol}$  ( $c$ ), and  $-52.27 \text{ kJ/mol}$  ( $c$ ) can be divided into four well separated groups. The results for the deepest ring and one of the chain structures are shown in Fig. 1. Both trimer and tetramer are symmetric ( $C_{nh}$ ) in their most stable structures with the hydroxyl groups arranged in planar rings. The binding energies of  $\Delta E = -73.44$  and  $-124.78 \text{ kJ/mol}$  are considerably larger than those of chainlike arrangements. For the larger systems planar ring structures are no longer energetically favored. The pentamer ( $\Delta E = -166.19 \text{ kJ/mol}$ ) shows an

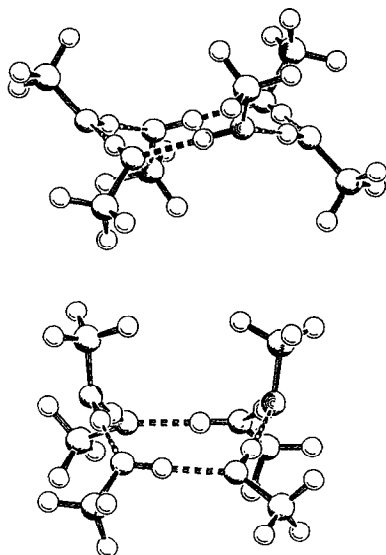


FIG. 2. The two lowest minimum configurations of the methanol hexamer. Upper panel, the lowest minimum structure of  $S_6$  symmetry and a binding energy of  $\Delta E = -204.13$  kJ/mol. Lower panel, a structure with  $C_2$  symmetry and a binding energy of  $\Delta E = -203.47$  kJ/mol.

asymmetric distorted configuration, while for the hexamer a variety of isomers occurs. There are two nearly degenerate isomers of  $S_6$  symmetry ( $\Delta E = -204.13$  kJ/mol) and  $C_2$  symmetry ( $\Delta E = -203.47$  kJ/mol) which are shown in

Fig. 2. Further stable structures which consist of rings with attached molecules or dimers are only a few kJ/mol less stable.

For the somewhat weaker PHH3 potential essentially the same minimum energy configurations are found. For the hexamer, these are the isomer of  $S_6$  symmetry ( $\Delta E = -162.45$  kJ/mol) and  $C_2$  symmetry ( $\Delta E = -162.44$  kJ/mol) which are closer together than those calculated for the OPLS potential.

## B. Simulated infrared spectra

In this section we discuss the simulated infrared spectra of small methanol aggregates. They were generated using the mixed classical/quantum mechanical procedure as is discussed previously. The thermal averaging over a canonical ensemble was carried out using the Monte Carlo technique described in Sec. II B. Figures 3(a) and 3(b) show as example the simulated absorption spectra for the cluster sizes  $n=4$  and 6 with the temperature varying from  $T=1$  to 100 K. One feature common to each of the series of spectra is the general tendency of broadening of the spectral lines with increasing temperature. For the lowest temperature ( $T=1$  K) the (inhomogeneous) widths of the lines range from 1 to 5  $\text{cm}^{-1}$ . Their positions are not shifted with respect to the frequencies obtained for rigid clusters at  $T=0$  K. These numbers can be found in our earlier publication.<sup>32</sup> For increasing temperatures, how-

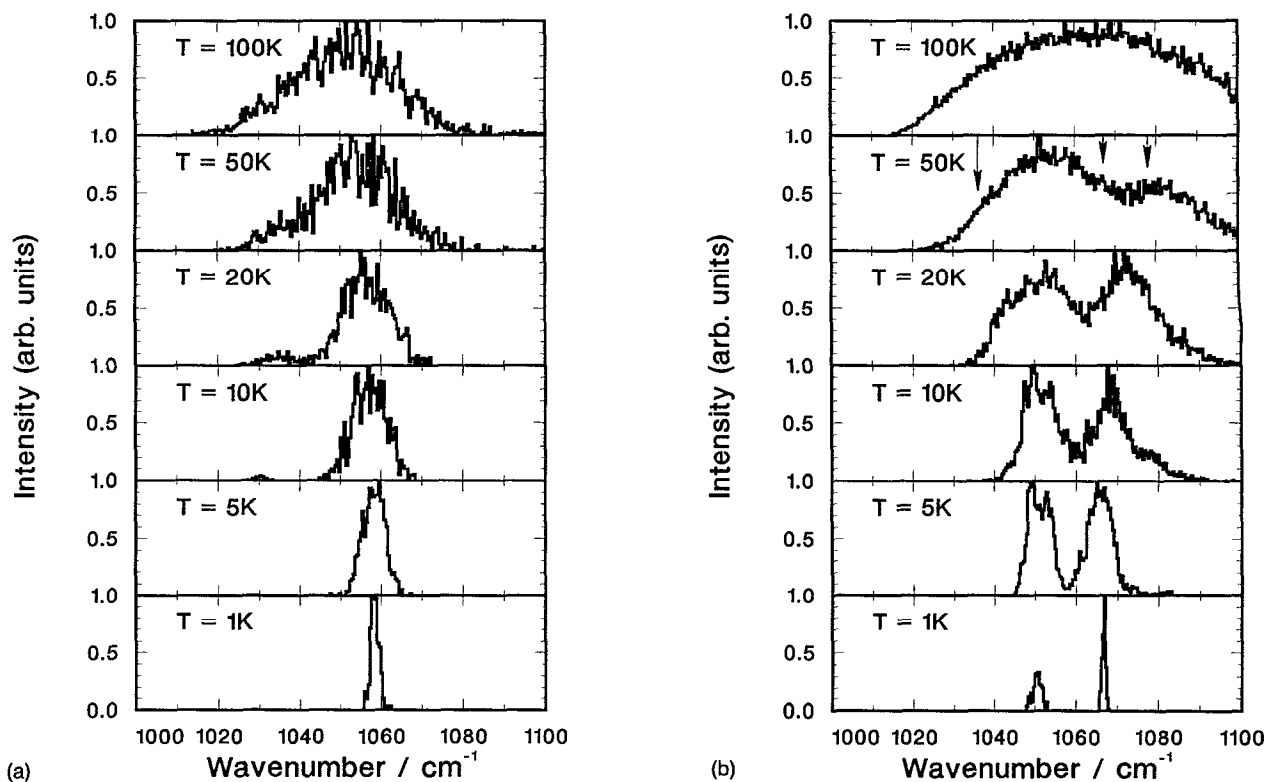


FIG. 3. (a) Simulated absorption spectra of the methanol tetramer at different temperatures in the region of the fundamental CO-stretching mode ( $\nu = 1033.5$   $\text{cm}^{-1}$ ). (b) Simulated absorption spectra of the methanol hexamer at different temperatures in the region of the fundamental CO-stretching mode ( $\nu = 1033.5$   $\text{cm}^{-1}$ ).

ever, the clusters become flexible and start to distort from their minimum energy configuration. Accordingly, the widths of the absorptions in the averaged infrared spectra are growing. At  $T=100$  K almost all characteristic spectroscopic patterns are lost and the simulated spectra show only very broad absorptions.

Interesting features can be observed in the spectra of the complexes exhibiting symmetric ring structures. At very low temperatures the spectra are still dominated by the symmetry of their respective minimum energy configurations. For the trimer ( $n=3$ ) and the tetramer ( $n=4$ ) the most stable isomers are of  $C_{nh}$  symmetry. Accordingly, the representations of the CO stretching vibrations ( $\nu_8$ ) of these aggregates can be reduced into  $\Gamma(\nu_8)=A'+E'$  for  $n=3$  and  $\Gamma(\nu_8)=A_g+B_g+E_u$  for  $n=4$ . This leads to only one absorption band in each of the spectra corresponding to an excitation of the infrared active  $E'$  and  $E_u$  mode, respectively. Similarly, for the most stable isomer of the methanol hexamer, the  $S_6$  symmetry considerably simplifies the spectrum. There the representation  $\Gamma(\nu_8)=A_g+E_g+A_u+E_u$  gives rise to only two infrared active modes ( $A_u$  and  $E_u$ ).

For finite temperatures the increasing nonrigidity of the clusters causes a gradual loss of symmetry. This may, in general, lead to different kinds of features in the spectra of the near symmetric complexes. (1) Excitations of vibrational modes which for  $T=0$  are infrared forbidden (denoted previously  $A'$  or with a subscript  $g$ ) appear in the spectra, and (2) the degeneracy of the  $E$  modes is removed. An example for the first phenomenon can be found in the simulated tetramer spectra depicted in Fig. 3(a). In addition to the  $E_u$  absorption a new peak shows up at  $T=10$  K in the region of  $1030\text{ cm}^{-1}$ . With increasing temperature it gains infrared activity until at around  $T=50$  K it fuses with the  $E_u$  peak due to the general broadening. Our frequency shift calculations show that this peak can be attributed to the excitation of a vibrational mode corresponding to the  $B_g$  mode of the  $C_{4h}$  symmetry of this complex. Similar observations are made for the simulated hexamer spectra shown in Fig. 3(b). Here the infrared intensity near  $1080\text{ cm}^{-1}$  found in the spectra for  $T=5$  and  $10$  K corresponds to the  $A_g$  mode of the isomer of  $S_6$  symmetry.

The expected splittings of absorption peaks corresponding to the excitation of  $E$  modes are hard to detect because this effect competes with the immense line broadening. Furthermore, fine details are obscured by the numerical noise of the Monte Carlo simulations. The  $E_u$  absorption in the hexamer spectra (near  $1050\text{ cm}^{-1}$ ) for  $T=5$  and  $10$  K is the only one clearly exhibiting a bimodal structure, while there are no clearly visible frequency splittings in the  $E_u$  absorption bands of the tetramer spectrum [see Fig. 3(a)]. For the pentamer which is not shown the opposite effect occurs. The three strongest lines of the spectrum at  $1051$ ,  $1055$ , and  $1061\text{ cm}^{-1}$  coalesce at  $20$  K to one broad line without structure.

Closer inspection of the hexamer spectra depicted in Fig. 3(b) reveals yet another interesting peculiarity. Aside from the effects related to the transition rules and to the

removal of degeneracies there are characteristic changes between  $T=20$ – $50$  K. The onset of absorption in the frequency regions  $1020$ – $1040\text{ cm}^{-1}$  and  $1080$ – $1100\text{ cm}^{-1}$  is stronger than the usual line broadening observed in the spectra for the other cluster sizes. Furthermore, there is a shift of the position of the outer peak from  $1070$  to  $1080\text{ cm}^{-1}$ . For these reasons, the changes might be interpreted as a transition where the hexamer crosses the potential barrier between its  $S_6$  symmetry configuration to the second most stable isomer of  $C_2$  symmetry. The latter bears strong infrared intensity in its  $A$  mode at  $1067\text{ cm}^{-1}$  and in its  $B$  modes at  $1036$  and at  $1078\text{ cm}^{-1}$  as shown in Fig. 6 of Ref. 32 and as arrows indicate in Fig. 3(b). The resulting change in the shape of the absorption bands may, therefore, be understood as an infrared signature of an isomerization transition. Since this transition is, however, not very sharp, we will examine the question of isomerization transitions more closely in Sec. III D where structural properties obtained in the simulations will be discussed.

### C. Comparison with experiment

The calculated spectra of the excitation of the CO stretching mode as function of temperature allow a direct comparison with the measured spectra of size selected clusters.<sup>27,28,51,52</sup> For smaller clusters up to the tetramer, two different methods for size selection have been used which lead to different internal temperatures. In the experiments of Refs. 27 and 51 the clusters are first size selected in a scattering process with atoms in which they are internally excited and then they interact with the laser for dissociation. In the experiments of Refs. 28 and 52 the interaction with the laser takes place before the size selection by scattering so that cold clusters are dissociated. Consequently the width of the dissociation spectra  $\Gamma$  is found to be  $\sim 4\text{ cm}^{-1}$  for  $n=2, 3$ , and  $4$ .<sup>52</sup> These results have to be compared with those obtained in the other experimental arrangement which give  $19/29\text{ cm}^{-1}$  for  $n=2$ ,  $13\text{ cm}^{-1}$  for  $n=3$ ,  $9\text{ cm}^{-1}$  for  $n=4$ ,  $7\text{ cm}^{-1}$  for  $n=5$ , and  $6/8\text{ cm}^{-1}$  for  $n=6$ , if we take the results of Table V of Ref. 27. If we interpret the measurements as essentially inhomogeneously broadened, we can derive temperatures by comparison with the Monte Carlo simulations of the last section. The results are temperatures of  $\sim 1$ – $5$  K for the experiments with small, cold clusters and values of  $50$  K ( $n=2$ ),  $20$  K ( $n=3$ ), and  $5$  K ( $n=4,5,6$ ) for the experiments with internally excited clusters. Even if we take into account that classical simulations with quantum mechanical calculations for the line shifts overestimate the widths<sup>53</sup> and thus underestimate the derived temperatures, the relative trends are reproduced as expected. The temperature difference which is obtained from the simulation for the two experimental data sets is largest for the dimer. Then this difference gradually decreases for the larger clusters. Such a behavior is certainly influenced by the increasing number of degrees of freedom for larger cluster sizes. In case of the dimer we have an independent measurement of the amount of energy which is deposited in the cluster. It gives for the

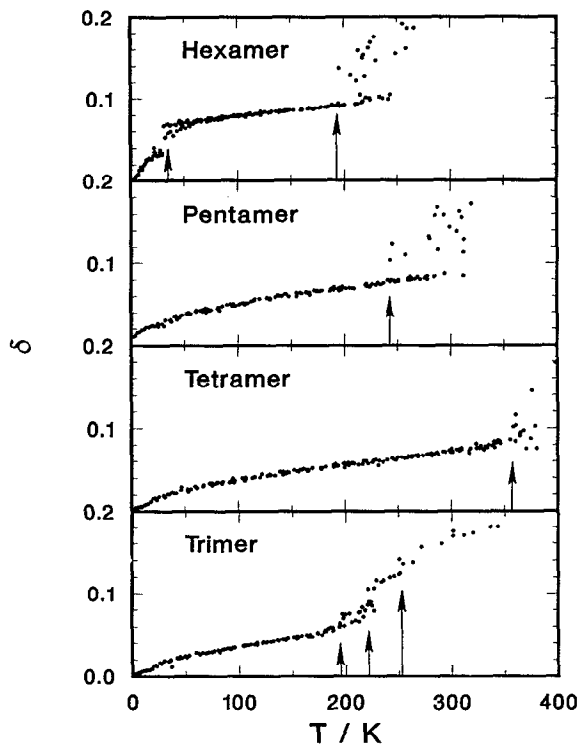


FIG. 4. The relative rms bond length fluctuations  $\delta_{\text{cm}}$  vs temperature  $T$  for  $n=3, 4, 5,$  and  $6$ . Arrows indicate the transition regions between different isomeric states for  $n=3$  at  $T \approx 197, 222,$  and  $253$  K, for  $n=4$  at  $T \approx 357$  K, for  $n=5$  at  $T \approx 243$  K and for  $n=6$  at  $T \approx 35$  and  $197$  K.

system under study  $259$  kJ/mol which corresponds to  $290$  K (Ref. 51) and which is indeed much larger than the value derived from the MC simulations.

In case of the hexamer we have additional information on the temperature of this cluster which is much more reliable. Aside from the width  $\Gamma$  which gives  $5$  K and which is probably too small, we definitely know from the measured spectrum that only the isomer of the lowest energy with  $S_6$  symmetry is present in the beam. Only this isomer exhibits a two band structure which is still present in the simulation at  $20$  K. At  $50$  K the influence of the next isomer of  $C_2$  symmetry comes into play. Thus we conclude that the temperature of the beam must be lower than the temperature of this isomeric transition. This value is still much lower than the one calculated on the basis of evaporative cooling.<sup>54</sup> On the other hand, these findings open up the possibility to use the dissociation spectra as clear indication for this phase transition. Experiments in this direction are under way.

#### D. Structural transitions

The calculated spectra presented in Sec. III B show evidence for a structural transition in methanol clusters. We now want to investigate these transitions in more detail. Let us consider first the relative rms bond length fluctuations  $\delta_{\text{cm}}$  as a function of temperature  $T$  in Fig. 4: An almost linear increase of  $\delta_{\text{cm}}$  with increasing  $T$  is an indication of the thermal expansion of the system. The mole-

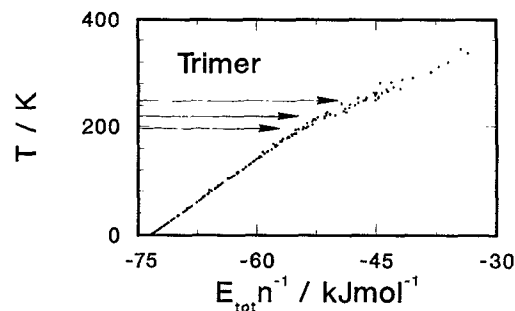


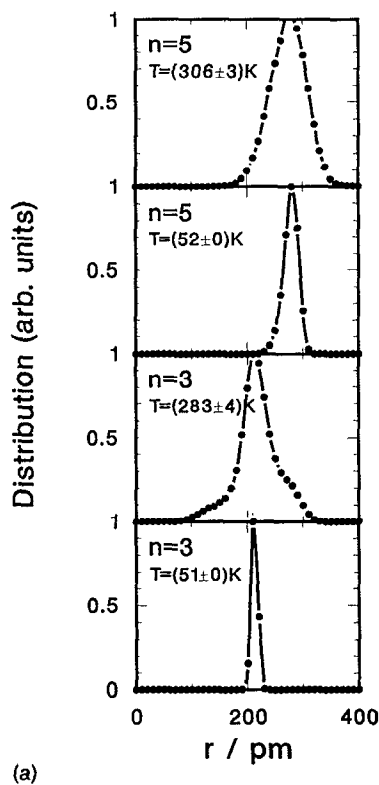
FIG. 5. The caloric curve of the methanol trimer. Arrows indicate the transition regions between different isomeric states of the trimer at  $T \approx 197, 222,$  and  $253$  K.

cules of the cluster vibrate about their well-defined minimum positions, but the system cannot pass over any potential barriers. An abrupt rise in  $\delta_{\text{cm}}$ , however, marks a structural transition. The newly accessed configuration space reveals further local minima on the corresponding potential hypersurface and the fluctuation between these minima accounts for the sharp rise in  $\delta_{\text{cm}}$ . In the caloric curve in Fig. 5 which is only shown for the trimer each "phase" can be attributed to a range with its own functional dependency of  $T$  upon  $E$ . For the bulk such ranges usually have well-defined separation points and Ehrenfest's classification of phase transitions makes direct use of the functional properties at these points. For clusters, however, there are no such well-defined separation points, because a phase transition smears out over a temperature range around the transition temperature due to finite size effects.<sup>55,56</sup> Considerable work has been done in characterizing the "phases" of a cluster,<sup>42,57,7</sup> the essential features of which have already been mentioned in the Introduction.

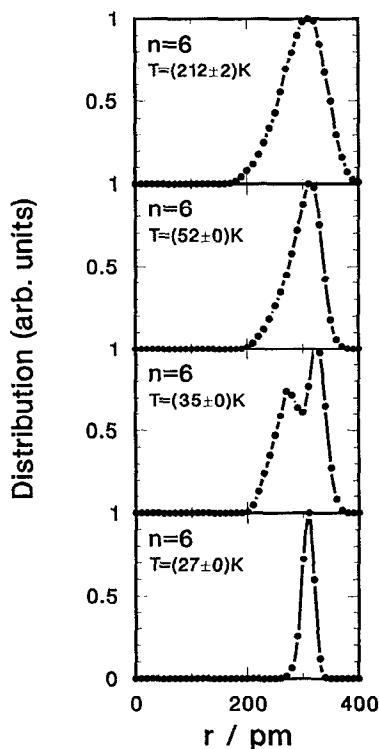
We will discuss the results for the different cluster sizes separately.

#### 1. Trimers

Six different minima were found for the trimer that can be energetically divided into four well separated groups consisting of rings and chains. Therefore we would ideally expect three different branches in the caloric curve and three abrupt rises in the  $\delta_{\text{cm}}$  curve. A close inspection of Fig. 4 (lowest panel) and Fig. 5 indicates that, indeed, these features can be found for the  $\delta_{\text{cm}}$ -curve at  $\sim 197, 222,$  and  $253$  K. The structural transitions at  $\sim 222$  and  $253$  K can also be observed in the caloric curve while the one at  $\sim 197$  K is not evident. Obviously our MD runs were too short so that the system could stay for the whole run in a single isomeric state or fluctuate between different isomeric states that were accessible, depending on the initial conditions. The structural transitions were also confirmed by visual inspection of trajectories at different temperatures  $T$  on our workstation computer, where the most significant change with rising  $T$  is the ring opening. At higher temperatures the system spent considerable simulation time in the linear chain structures as are described in Sec. III A. This is further confirmed by the distribution of distances of



(a)



(b)

FIG. 6. (a) The distribution of bond lengths from the center of mass of each molecule to the center of mass of the cluster for  $n=3$  and 5 at different temperatures. (b) The distribution of bond lengths from the center of mass of each molecule to the center of mass of the cluster for  $n=6$  at different temperatures.

the center-of-mass of the molecules to the center-of-mass of the cluster which are displayed in Fig. 6. The lowest panel of Fig. 6(a) shows a single narrow peak reflecting the rigid ring structure at 51 K. The next panel shows the results taken at 283 K. Around the broad peak in the middle, two peaks have appeared which reflect the fluctuating chain structure of the higher lying isomers.

## 2. Tetramers and pentamers

The  $\delta_{\text{cm}}$ -curves of the tetramer and pentamer show a qualitatively new feature: No sharp rise of  $\delta_{\text{cm}}$  can be observed, but rather a broadening in their distribution that becomes larger with increasing temperature. We again invoke nonthermal behavior of the systems to explain this peculiarity. For longer MD-runs we expect unique values of  $\delta_{\text{cm}}$ , independent of initial conditions. Therefore we interpret this feature as a structural transition for the tetramer at  $T \approx 357$  K and for the pentamer at  $T \approx 243$  K. No distinct branches can be seen in the caloric curves and consequently an attribution of single isomeric states is not possible. Instead we again visually inspected the dynamics of several trajectories. While for the trimer with rising temperature the ring opening is the most prominent characteristic, tetramer and pentamer spent most of their time in ring structures even at high temperatures. This is also confirmed by the  $h(r)$  curves in the upper part of Fig. 6(a) that show only homogeneous broadening for the pentamer with rising temperature compared with increasing shoulders in the distribution of the trimer, indicating the statistical weight of their linear structures in our simulations.

## 3. Hexamers

The two energetically lowest minima that are well separated from the other structures characterize the first structural transition of the hexamer. After a sharp increase of  $\delta_{\text{cm}}$  up to  $T \approx 35$  K the curve flattens drastically, signaling that the structural transition has taken place and that there is rapid fluctuation between the two isomeric states. A second "phase transition" showing similar features in the curve as for the tetramer and pentamer, occurs at  $T \approx 197$  K. No attribution of special isomeric states can be made for the second structural transition. Fingerprints of the structures participating in the first structural transition, however, can be observed in the  $h(r)$  plots in Fig. 6(b). Up to a temperature slightly below 35 K only one peak at  $r \approx 310$  pm can be seen, characterizing the lowest minimum structure of  $S_6$  symmetry. In a small temperature range above, however, a double peak structure at  $r \approx 280$  and 330 pm can be observed with slightly more intensity in the second peak. This double peak structure can be attributed to the "boat configuration" of the hexamer of  $C_2$  symmetry. The system can surmount the barrier between the two local minima and spends considerable simulation time in the boat structure. At higher temperatures the fluctuations between the two isomeric states become more frequent and only one unsymmetric and broad peak can be seen in the  $h(r)$  curve.



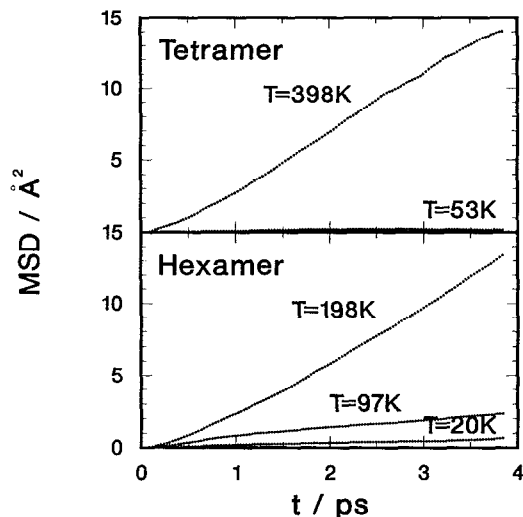


FIG. 7. The mean square displacements vs time at different temperatures  $T$  for  $n=4$  and 6. For the tetramer the lower curve at  $T=53$  K indicates a solidlike state of the cluster while the upper curve at  $T=398$  K indicates a liquidlike state. Three curves are plotted for the hexamer; the two lower curves at  $T=20$  and 97 K indicate a solidlike state, and the one at  $T=198$  K a liquidlike state. The curves were calculated over 156 independent time origins.

In order to test the sensitivity of these results to the potential model, the calculations are repeated using the PHH3 potential. Again both transitions are observed. The first one between the  $S_6$  and the  $C_2$  isomer occurs at 18 K, which is lower than the value found for the OPLS potential. The second one occurs at 181 K quite close to the OPLS value. Apparently the low temperature isomeric transition is more sensitive to the choice of the potential surface than is the high temperature transition. But the gross features are qualitatively the same.

In concluding this section we note that with rising  $n$  from 4 over 5 to 6 the temperature of the final structural transitions decreases. This is in contrast to what has been found for clusters up to now. In addition we note that the melting temperature of the bulk at  $T=175.2$  K is well below the above mentioned transition temperatures. This result is a consequence of the unique binding properties of these clusters which exhibit a maximum of relative binding energies for the tetramer because of the cooperativity effect in hydrogen bonding.<sup>29</sup>

In order to prove whether the clusters are liquid- or solidlike, we have also calculated the MSD as a function of time. The results are shown in Fig. 7. For the tetramer, the curve obtained for  $T=53$  K with a horizontal line is solidlike, while at 398 K the straight line with a finite slope is as expected liquidlike. For the hexamer, three curves have been calculated at 20, 97, and 198 K. The first two curves are still in the regime of the solidlike behavior and confirm the interpretation of an isomeric transition between the  $S_6$  and the  $C_2$  structure. Note that the behavior of the cluster before the transition is solidlike while afterwards it is floppy-solidlike.<sup>7</sup> The third curve corresponds already to liquidlike behavior and indicates a multistate isomerization

similar to the transitions found for the tetramer and pentamer.

## E. Concluding remarks

In the MC and MD simulations of the structure and energetics of small methanol clusters different kinds of isomeric transitions have been observed. The trimer passes from the lowest energy, rigid configuration, a symmetric ring, over several chain configurations into a nonrigid open chain configuration at temperatures about  $T=197$ , 222, and 253 K. For the tetramer and pentamer a transition occurs between the ring structure at low temperatures and a rapidly fluctuating ring at much higher temperatures about  $T=357$  and 243 K, respectively. It is noted that these transitions take place at higher temperatures than that of the bulk and are largest for the tetramer, a clear manifestation of the strong cooperative hydrogen bonding in these species.

A specially interesting case is the hexamer. First there is a pure isomeric transition at about 35 K between the two energetically lowest isomers of  $S_6$  and  $C_2$  symmetry. According to the nondiffusive MSD curves the behavior of the cluster below this transition temperature is solidlike, whereas above it is floppy-solidlike. Similar results have also been obtained in the analysis of NaCl and KCl tetramers.<sup>6,7</sup> The transition to the liquidlike behavior then occurs at much higher temperatures at about 197 K in the same way as has been found for the tetramer and the pentamer. The signature of the isomeric transition at 35 K can be found unambiguously in the simulated IR spectra. In the experiment, only the two peak structure of the  $S_6$ -isomer is observed, a clear indication that the beam temperature is below the transition temperature. Test calculations for a different potential surface indicate that the pure isomeric transition depends more sensitively on the potential than the transition to the liquidlike behavior.

## ACKNOWLEDGMENT

The financial support from the Deutsche Forschungsgemeinschaft in the Schwerpunktprogramm Molekulare Cluster is gratefully acknowledged.

- <sup>1</sup> R. S. Berry, T. L. Beck, H. L. Davies, and J. Jellinek, *Adv. Chem. Phys.* **70**, 74 (1988).
- <sup>2</sup> J. Jortner, D. Scharf, and U. Landman, in *Elemental and Molecular Clusters*, edited by G. Benedek, T. P. Martin, and G. Pacchioni (Springer, Berlin, 1988), p. 148.
- <sup>3</sup> R. S. Berry, in *The Chemical Physics of Atomic and Molecular Clusters*, edited by G. Scoles (North-Holland, Amsterdam, 1990), p. 23.
- <sup>4</sup> J. Jortner, D. Scharf, N. Ben-Horin, U. Even, and U. Landman, in *The Chemical Physics of Atomic and Molecular Clusters*, edited by G. Scoles (North-Holland, Amsterdam, 1990), p. 43.
- <sup>5</sup> T. P. Martin, *Phys. Rep.* **95**, 167 (1983).
- <sup>6</sup> A. Heidenreich, J. Jortner, and I. Oref, *J. Chem. Phys.* **97**, 197 (1992).
- <sup>7</sup> J. P. Rose and R. S. Berry, *J. Chem. Phys.* **96**, 517 (1992).
- <sup>8</sup> A. Buffat and J. P. Borel, *Phys. Rev. A* **13**, 2289 (1976).
- <sup>9</sup> S. Leutwyler and J. Bösinger, *Chem. Rev.* **90**, 489 (1990).
- <sup>10</sup> N. Ben-Horin, U. Even, J. Jortner, and S. Leutwyler, *J. Chem. Phys.* **97**, 5296 (1992).
- <sup>11</sup> N. Ben-Horin, U. Even, and J. Jortner, *J. Chem. Phys.* (to be published).

- <sup>12</sup>R. D. Etters, K. Flurchik, R. P. Pan, and V. Chandrascharan, *J. Chem. Phys.* **75**, 929 (1981).
- <sup>13</sup>G. del Mistro and A. J. Stace, *Chem. Phys. Lett.* **171**, 381 (1990).
- <sup>14</sup>G. J. Tsai and K. D. Jordan, *J. Chem. Phys.* **95**, 3850 (1991).
- <sup>15</sup>L. S. Bartell and Jian Chen, *J. Phys. Chem.* **96**, 8801 (1992).
- <sup>16</sup>Q. Zhang and V. Buch, *J. Chem. Phys.* **92**, 5004 (1990).
- <sup>17</sup>F. M. Beniere, B. Rousseau, A. H. Fuchs, M. F. de Feraudy, and G. Torchet, in *Physics and Chemistry of Finite Systems*, edited by P. Jena *et al.* (Kluwer, Dordrecht, 1992), p. 363.
- <sup>18</sup>G. Torchet, J. Farges, M. F. de Feraudy, and B. Raoult, in *The Chemical Physics of Atomic and Molecular Clusters*, edited by G. Scoles (North-Holland, Amsterdam, 1990), p. 513.
- <sup>19</sup>L. S. Bartell and T. S. Dibble, *J. Phys. Chem.* **95**, 1159 (1991).
- <sup>20</sup>R. E. Miller, R. O. Watts, and A. Ding, *Chem. Phys.* **83**, 155 (1984).
- <sup>21</sup>D. Eichenauer and R. J. LeRoy, *J. Chem. Phys.* **88**, 2898 (1988).
- <sup>22</sup>J. A. Barnes and T. E. Gough, *J. Chem. Phys.* **86**, 6012 (1987).
- <sup>23</sup>G. Cardini, V. Schettino, and M. L. Klein, *J. Chem. Phys.* **90**, 4441 (1989).
- <sup>24</sup>M. A. Kmetc and R. J. LeRoy, *J. Chem. Phys.* **95**, 6271 (1991).
- <sup>25</sup>N. Ben-Horin, Dar Bahatt, U. Even, and J. Jortner, *J. Chem. Phys.* (to be published).
- <sup>26</sup>X. J. Gu, D. J. Levandier, B. Zhang, G. Scoles, and D. Zhuang, *J. Chem. Phys.* **93**, 4898 (1990).
- <sup>27</sup>U. Buck, X. J. Gu, C. Lauenstein, and A. Rudolph, *J. Chem. Phys.* **92**, 6017 (1990).
- <sup>28</sup>F. Huisken and M. Stemmler, *Chem. Phys. Lett.* **144**, 391 (1988).
- <sup>29</sup>L. A. Curtiss and M. Blander, *Chem. Rev.* **88**, 827 (1988).
- <sup>30</sup>W. L. Jorgensen, *J. Phys. Chem.* **90**, 1276 (1984).
- <sup>31</sup>A. Serrallach, R. Meyer, and H. H. Günthard, *J. Mol. Spectrosc.* **52**, 94 (1974).
- <sup>32</sup>U. Buck and B. Schmidt, *J. Chem. Phys.* **98**, 9410 (1993).
- <sup>33</sup>G. Pálkás, E. Hawlicka, and K. Heinzinger, *J. Phys. Chem.* **91**, 4334 (1987).
- <sup>34</sup>N. Metropolis, A. W. Rosenbluth, M. N. Rosenbluth, A. H. Teller, and E. Teller, *J. Chem. Phys.* **21**, 1087 (1953).
- <sup>35</sup>H. Goldstein, *Classical Mechanics* (Addison-Wesley, Reading, 1980).
- <sup>36</sup>M. P. Allen and D. J. Tildesley, *Computer Simulations of Liquids* (Clarendon, Oxford, 1987).
- <sup>37</sup>D. J. Evans, *Mol. Phys.* **34**, 317 (1977).
- <sup>38</sup>D. J. Evans and S. Murad, *Mol. Phys.* **34**, 327 (1977).
- <sup>39</sup>C. W. Gear, *Numerical Initial Value Problems in Ordinary Differential Equations* (Prentice-Hall, Englewood Cliffs, 1971).
- <sup>40</sup>H. J. C. Berendsen and W. F. van Gunsteren, in *Proceedings of the Enrico Fermi Summer School*, Bologna, 1966 (Varenna, 1985).
- <sup>41</sup>R. G. Gilbert and S. C. Smith, *Theory of Unimolecular and Recombination Reactions* (Blackwell, Oxford, 1990).
- <sup>42</sup>J. Jellinek, T. L. Beck, and R. S. Berry, *J. Chem. Phys.* **84**, 2783 (1986).
- <sup>43</sup>T. L. Beck, J. Jellinek, and R. S. Berry, *J. Chem. Phys.* **87**, 545 (1987).
- <sup>44</sup>F. G. Amar and R. S. Berry, *J. Chem. Phys.* **85**, 5943 (1986).
- <sup>45</sup>S. K. Schiferl and D. C. Wallace, *J. Chem. Phys.* **83**, 5203 (1985).
- <sup>46</sup>F. A. Lindemann, *Phys. ZS.* **11**, 609 (1910).
- <sup>47</sup>A. D. Buckingham, *Proc. R. Soc. London, Ser. A* **248**, 169 (1958).
- <sup>48</sup>A. D. Buckingham, *Trans. Faraday Soc.* **56**, 753 (1960).
- <sup>49</sup>U. Buck and B. Schmidt, *J. Mol. Liquids* **46**, 181 (1990).
- <sup>50</sup>H. B. Schlegel, S. Wolfe, and F. Bernardi, *J. Chem. Phys.* **67**, 4181 (1977).
- <sup>51</sup>U. Buck, Ch. Lauenstein, and A. Rudolph, *Z. Phys. D* **18**, 181 (1991).
- <sup>52</sup>F. Huisken and M. Stemmler, *Z. Phys. D* **24**, 277 (1992).
- <sup>53</sup>L. Ojamäe, J. Tegenfeldt, J. Lindgren, and K. Hermansson, *Chem. Phys. Lett.* **195**, 97 (1992).
- <sup>54</sup>C. E. Klots, *Z. Phys. D* **21**, 335 (1991).
- <sup>55</sup>K. Binder, in *Finite Size Scaling and Numerical Simulation of Statistical Systems* (World Scientific, Singapore, 1990).
- <sup>56</sup>D. P. Landau, in *Finite Size Scaling and Numerical Simulation of Statistical Systems* (World Scientific, Singapore, 1990).
- <sup>57</sup>S. Sawada and S. Sugano, *Z. Phys. D* **14**, 247 (1989).